Contents lists available at ScienceDirect

Annual Reviews in Control

journal homepage: http://ees.elsevier.com

Adaptive-learning model predictive control for complex physiological systems: Automated insulin delivery in diabetes

Mohammad Reza Askari [a], Iman Hajizadeh [a], Mudassir Rashid [a], Nicole Hobbs [a], Victor M. Zavala [c], Ali Cinar [a,b,*]

[a] Department of Chemical and Biological Engineering, Illinois Institute of Technology, Chicago, IL 60616, United States
[b] Department of Biomedical Engineering, Illinois Institute of Technology, Chicago, IL 60616, United States
[c] Department of Chemical and Biological Engineering, University of Wisconsin-Madison, Madison, WI 53706, United States

ARTICLE INFO

Article history:
Received 7 May 2020
Received in revised form 6 October 2020
Accepted 8 October 2020
Available online xxx

Keywords
Adaptive learning
Dynamic principal component analysis
Insulin delivery system
Latent variable regression
Model predictive control

ABSTRACT

An adaptive-learning model predictive control (AL-MPC) framework is proposed for incorporating disturbance prediction, model uncertainty quantification, pattern learning, and recursive subspace identification for use in controlling complex dynamic systems with periodically recurring large random disturbances. The AL-MPC integrates online learning from historical data to predict the future evolution of the model output over a specified horizon and proactively mitigate significant disturbances. This goal is accomplished using dynamic regularized latent variable regression (DrLVR) approach to quantify disturbances from the past data and forecast their future progression time series. An enveloped path for the future behavior of the model output is extracted to further enhance the robustness of the closed-loop system. The controller set-point, penalty weights of the objective function, and constraints criteria can be modified in advance for the expected periods of the disturbance effects. The proposed AL-MPC is used to regulate glucose concentration in people with Type 1 diabetes by an automated insulin delivery system. Simulation results demonstrate the effectiveness of the proposed technique by improving the performance indices of the closed-loop system. The MPC algorithm integrated with DrLVR disturbance predictor has compared to MPC reinforced with dynamic principal component analysis linked with K-nearest neighbors and hyper-spherical clustering (k-means) technique. The simulation results illustrate that the AL-MPC can regulate the glucose concentrations of people with Type 1 diabetes to stay in the desired range (70–180) *mg/dL* 84.4% of the time without causing any hypoglycemia and hyperglycemia events.

1. Introduction

Data analytics, machine learning (ML), and artificial intelligence (AI) have extended closed-loop control performance in complex systems. Our earlier work leveraged knowledge-based systems (KBS) operating for retuning or restructuring control systems in real-time (Basila Jr, Cinar, & Stefanek, 1989; Kendra, Basila, & Cinar, 1997). The object-rule hybrid KBS recognized when the control system would have degradation in performance as process operating conditions changed, and modified the controller automatically (Basila Jr et al., 1989). This framework was extended to supervise multivariable system operation and used robust control techniques to retune or restructure the control system automatically (Kendra, Basila, & Cinar, 1994; 1997). Multivariate statistical techniques were linked with KBS to integrate multivariate process monitoring and fault diagnostics by using G2 by Gensym, Inc. (Gensym, 1996), a commercial real-time KBS development system for process operations (Tatara & Cinar, 2002). This framework was extended to control system performance assessment and modification (Schäfer & Cinar, 2004). The advent of agent-based systems enabled distributed AI implementation, leading to hierarchical agent-based supervision systems with distributed monitoring, diagnosis, and control functionality to supervise and regulate distributed processes for comprehensive multi-layered monitoring, diagnosis, and control unit, section and plant level operation (Perk, Shao, Teymour, & Cinar, 2012; Perk, Teymour, & Cinar, 2011; Tatara, North, Hood, Teymour, & Cinar, 2005). The data analytics, ML, and AI experience we gained in this journey provided the opportunity to apply these techniques to automated drug delivery, focusing on automated insulin delivery to people with diabetes with a multivariable artificial pancreas (mAP).

* Corresponding author at: Department of Chemical and Biological Engineering, Illinois Institute of Technology, Chicago, IL 60616, United States.
E-mail addresses: maskari@hawk.iit.edu (M.R. Askari); ihajizad@hawk.iit.edu (I. Hajizadeh); mrashid3@iit.edu (M. Rashid); nhobbs@hawk.iit.edu (N. Hobbs); victor.zavala@wisc.edu (V.M. Zavala); cinar@iit.edu (A. Cinar)

https://doi.org/10.1016/j.arcontrol.2020.10.004
1367-5788/

The control of complex systems with nonlinear structure, unmodeled dynamics, and unknown time-varying parameters is challenging. The presence of measurement errors and artifacts, unmeasurable and unknown disturbances, and time-varying delays provide additional obstacles. Control system formulations based on time-invariant models cannot accurately capture these process dynamics and control them effectively. Hence, the effectiveness of non-adaptive controllers is questionable when such systems are subjected to large-magnitude disturbances while their operating points are varying over broad regions. To address this issue, adaptive system identification was widely used to update the controller parameters based on the identified model recursively. The closed-loop implementation of system identification has shown to be rather tricky due to the existence of the correlation between input and unmeasurable noise disturbances (Lennart, 1999). In recent years, subspace identification techniques have attracted attention over error prediction-based techniques due to their ability to identify minimal models (Lennart, 1999; Verhaegen, 1993). Chou and Verhaegen (1997) also addressed the problem of identifying multivariable finite-dimensional linear time-invariant systems from open- or closed-loop data and with the presence of correlation in the noise processes. The advances in system identification for closed-loop data were achieved by utilizing the principal component analysis to consistently identify a subspace-based model from the closed-loop input-output data subject to errors-in-variables (Wang & Qin, 2002). However, identified models from subspace systems identification algorithms are not as accurate as those estimated from the error prediction methods (Qin, 2006). Hence, incorporating auxiliary methods such as latent variable-based regression or unsupervised learning methods can significantly enhance the performance of the output predictions and, consequently, the effectiveness of the controller.

Model predictive control (MPC) gained popularity in many applications due to its inherent ability to efficiently handle complex multivariable systems and constraints (Ganesh, Edgar, & Baldea, 2016; Garcia, Prett, & Morari, 1989; Garcia-Tirado, Corbett, Boiroux, Jørgensen, & Breton, 2019; Hajizadeh, Rashid, & Cinar, 2019b; Mayne, 2014; Mesbah, Paulson, Lakerveld, & Braatz, 2017; Moharir, Pourkargar, Almansoori, & Daoutidis, 2018; Perea-Lopez, Ydstie, & Grossmann, 2003; Rawlings & Mayne, 2009; Zavala & Biegler, 2009). MPC algorithms cast an optimization problem to estimate the future evolution of system outputs and minimize an objective function over a finite-time horizon by using a dynamic model of the process and constraints. The optimal values of the manipulated variables with respect to the specified performance index are determined and implemented. MPC formulations are not restricted by the type of model, objective function, or constraints. However, model mismatch, the formulation of the objective function, system constraints, and unknown random disturbances affect the performance of MPC (Forbes, Patwardhan, Hamadah, & Gopaluni, 2015; Kumar et al., 2019a; 2018; 2019b).

In standard implementation of MPC, the deterministic representation of random disturbances is used to calculate control actions. In other words, the projection acts as a summarizing statistic (usually expected value) of the entire disturbance uncertainty space. Since ordinary MPC is not able to handle disturbances that cannot be well-represented by most likely forecasts, stochastic MPC (sMPC) formulations have been developed in recent years (Kumar et al., 2019a; 2018; 2019b; Mesbah, 2016). sMPC utilizes historical data to form uncertainty characterizations of the model disturbances. These characterizations are used to generate the most probable scenarios for the evolution of the outputs over the specified prediction horizon. Hence, sMPC presents a methodical framework to guarantee control objectives and address probabilistic constraints caused by uncertainties (Mesbah, 2016). Augmented past data can be leveraged into probabilistic learning techniques, namely maximum likelihood, to be incorporated with MPC to forecast and generate different scenarios (Ripaccioli, Bernardini, Di Cairano, Bemporad, & Kolmanovsky, 2010). In order to improve the output forecasts over the prediction horizon, most probable scenarios should be generated in the controller for process disturbances. The objective is to quantify significant disturbances and forecast their future occurrence by using historical data and ML techniques. Moreover, the set-point of the controller (reference trajectory), adjustable weights in the objective function, and the system constraints can be appropriately modified in advance for the expected duration of the disturbance effects ()Hajizadeh, Askari, Kumar, Zavala, and Cinar, 2020 (in press; Hajizadeh et al., 2019a).

In this work, data analytics, ML, and AI are integrated with adaptive MPC to regulate a nonlinear process with time-varying parameters subject to periodic large magnitude disturbances. A novel approach is proposed to extract information from historical data and predict likely disturbances and their characteristics, followed by feeding the refined knowledge to our adaptive MPC based on recursively updated models and dynamically adjustable constraints. Disturbance prediction based on dynamic regularized latent variable regression (DrLVR) has been utilized for disturbance forecasting, uncertainty quantification, and the system output prediction from periodic historical data. Latent variable regression (LVR) a statistical approach for latent structure extraction. It aims to establish a relationship between variables in such a way that the maximum correlation across two sets of measured variables and the variation of each component is obtained. Hence, LVR takes into account the benefits of partial least squares regression (PLSR) and canonical correlation analysis (CCA) (Loehlin & Beaujean, 2016; Velu & Reinsel, 2013; Zhou, Li, Song, & Qin, 2016; Zhu, Qin, & Dong, 2020). Based on the method suggested in Zhu, Liu, and Qin (2017) for extracting the inherent dynamic structures in the data by using dynamic inner principal component analysis (DPCA), a latent variable-based approach that generates a vector autoregressive (VAR) model from the lagged matrices of input and output variables was proposed (Zhu et al., 2020). DrLVR is robust to co-linearity between the variables of process data and singularity issues in calculating the inverse of the squared process data matrix. Dynamic inferential monitoring with DPCA (Zhu et al., 2017) was proposed for monitoring the future process variables and fault diagnosis before adjusting the process variables. Historical data can also be used to identify the behaviors and patterns of the underlying system for control system adjustment. Incorporating the online prediction of unknown disturbances from the historical data using DrLVR can improve the control system performance by mitigating the effects of impending disturbances more effectively.

A qualitative trend analysis (QTA) method based on outputs measurements is also used to identify rapid divergences from the desired trajectories stemming from significant disturbances in real-time (Cheung & Stephanopoulos, 1990; Maurya, Rengaswamy, & Venkatasubramanian, 2005; Samadi et al., 2018; 2017). QTA feature extraction scheme provides information about the rate and the shape of variations in outputs measurements to adjust the controller when the presence of significant disturbances is detected (Hajizadeh et al., 2019a).

The performance of the proposed approach is tested by regulating the blood glucose concentrations (GC) in people with Type 1 diabetes (T1D) by automated insulin delivery with a multivariable artificial pancreas (mAP) system (Hajizadeh et al., 2019b; Hajizadeh et al., 2019c; Reddy et al., 2016; Thabit & Hovorka, 2016). The mAP receives subcutaneous GC data from a continuous glucose monitoring (CGM) system and physiological data from a wristband with several sensors. Insulin doses recommended by the mAP are infused to subcutaneous tissue by an insulin pump (Fig. 1). The wristband sensors have a negligible delay with respect to GC readings. CGM reports blood GC with 5–10 min of delay caused by blood diffusion from the vascular system to subcutaneous tissue. The delay in insulin action can be

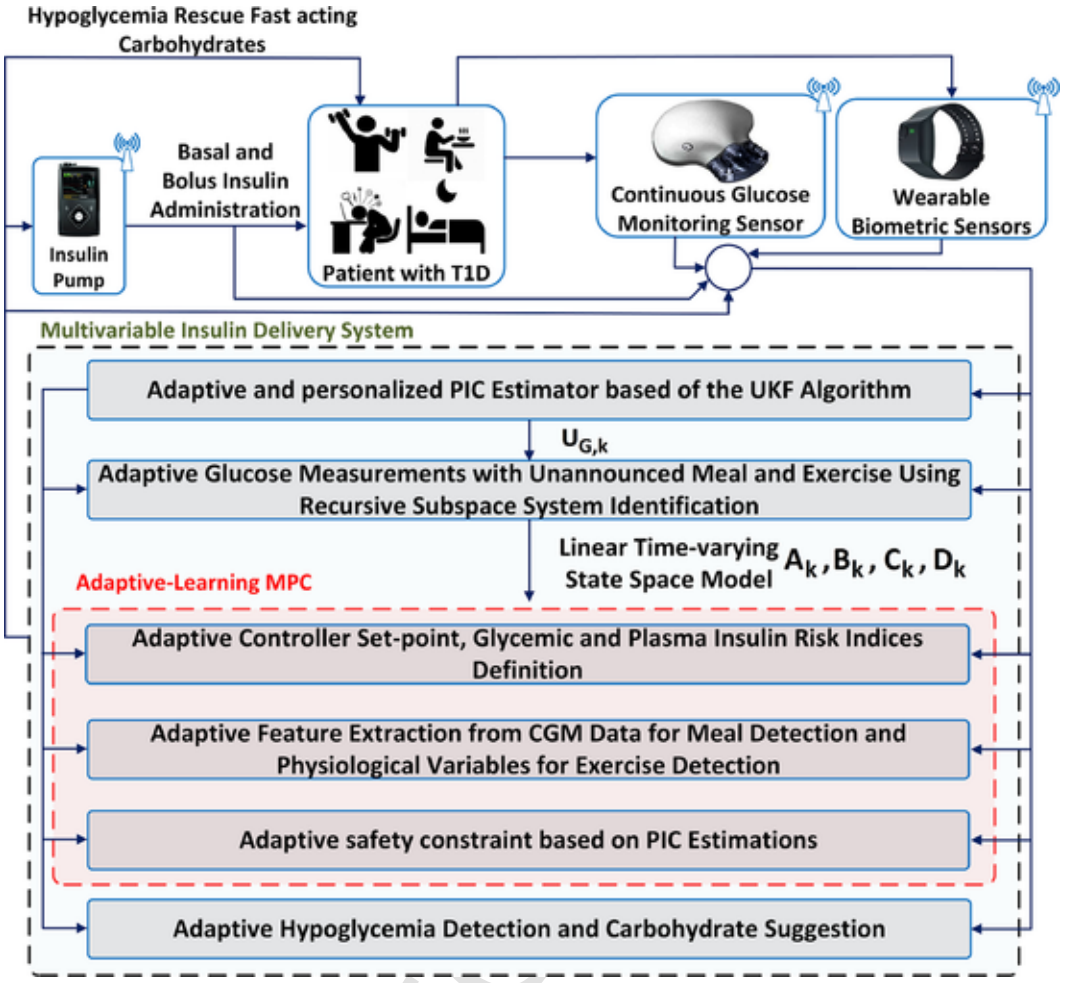

Fig. 1. The mAP with AL-MPC for the regulation of GC of people with T1D (Hajizadeh, Samadi, Sevil, Rashid, & Cinar, 2019d).

20–40 min from the infusion time by the pump. Biological processes are complex dynamical systems with many uncertainties and significant exogenous disturbances that render their modeling and control a challenging task(Sevil et al., 2019; 2020). The human body, a time-varying system with nonlinear behavior, is affected by several random and unknown disturbances. Its representation with fixed-parameter linear models and regulation with controllers that use such models had limited success.

Automated insulin delivery systems are expected to regulate GC to keep it in the normal (euglycemic) range (70–180 mg/dL), and recent clinical experiments reported that the GC is kept in this range about 70% of the time with fewer hypoglycemic (BC $< 70\,md/dL$) and hyperglycemic (GC $> 180\,md/dL$) events compared to manual insulin adjustments by the user. Large periodic disturbances such as meals and physical activity can deteriorate the controller performance and cause hypoglycemia or hyperglycemia. Meals increase glucose levels while the effects of physical activities depend on the type, intensity, and duration of the activity. Low- and medium-intensity aerobic physical activities increase insulin sensitivity and cause rapid reductions in GC, and can activate counter-regulatory hormones (Breton, 2008; Galassetti & Riddell, 2013; Riddell & Perkins, 2009; Zecchin et al., 2013). Nevertheless, high-intensity exercise may cause hyperglycemia. The mAP framework enabled the use of physiological signals to detect the presence of physical activities and estimate their types and intensities. Hence, physical activities become measurable disturbances and provide feedforward control. Thus, mAP has a better ability to avoid hypoglycemia or hyperglycemia as it can detect physical activity from the measured physiological variables (Sevil et al., 2020; Turksoy, Bayrak, Quinn, Littlejohn, & Cinar, 2013a; Turksoy, Quinn, Littlejohn, & Cinar, 2013b), well before the effect of physical activities manifest itself in the CGM data. We have also developed meal detection and bolus-insulin-infusion computation algorithms and integrated them to the mAP system.

The performance of the mAP controller can be further improved by long-horizon prediction of likely disturbances to make the controller ”proactively” regulate the GC in addition to ”actively” administering basal and bolus insulin the adaptive MPC of the mAP. Disturbance (meal and physical activity) prediction over longer time horizons is achieved by data analytics, and ML of historical data. These predictions are then incorporated into the adaptive MPC to develop an mAP with a learning system, which is the topic of this work. This system is called the adaptive learning MPC (AL-MPC), and its modules are outlined in Fig. 1.

The main contributions of this study are:

- Historical data analytics with a DrLVR algorithm to estimate the future evolution of the process output with respect to estimated disturbances on a specified long prediction horizon. Upper and lower bounds of these disturbances and their expected values and times of occurrence are predicted.
- Developing a method for constructing an enveloped path of future values of outputs and embedding into the optimization problem in order to further enhance the robustness of the closed-loop system against worst case scenarios.

- Incorporating criteria and algorithms in MPC for modifying setpoint values and penalty weights in the optimization problem over the prediction horizon. This modification better addresses the delayed feedback response of the closed-loop system and improves its performance in the presence of time-varying delay.

The performance of the mAP with AL-MPC is evaluated and illustrated with simulations conducted by using a multivariable glucose-insulin-physiological variables simulator (mGIPsim) for T1D developed at Illinois Institute of Technology (Rashid et al., 2019). This unique simulator provides, in addition to GC, physiological variables that represent some of the wristband signals and energy expenditure (EE) estimates derived from wristband signals as outputs, enabling testing of the mAP *in silico*. Simulation results show a significant improvement in the performance of the mAP system with respect to an MPC without the learning ability, and the proposed algorithm illustrates potential progress in the development of fully automated mAP system.

The remainder of this paper is structured as follows. Recursive predictor-based subspace identification (RPBSID), variable prediction using DrLVR, and adaptive-learning model predictive control (AL-MPC) are described and discussed in the Problem Formulation and Methods section. Simulation results with mGIPsim are presented in the Results section. The interpretation and comparison of the results with various control systems are provided in the Discussion section. Conclusions are stated in the last section.

2. Problem formulation and methods

This section presents a summary of the recursive subspace identification method for adaptively identifying state-space dynamics, the forecast of the process disturbances using the DrLVR technique, and the formulation of the AL-MPC.

2.1. Recursive subspace model identification

Extracting a reliable and stable model is crucial for designing the MPC controller in the insulin delivery system. A first-principles compartment model known as Hovorka's model, is widely used to describe the insulin-glucose dynamics in people with T1D. The nonlinear dynamic model consists of nine ordinary differential equations that model the GC dynamics, the subcutaneous insulin injection, and the dynamic of glucose transport from plasma to interstitial (subcutaneous) tissues (Hovorka et al., 2004).

A predictor-based subspace identification method is employed to estimate the behavior of glucose-insulin dynamics in a time-varying linear model format. The identification algorithm is incorporated with the constrained optimization problem to ensure the stability of the identified model (Hajizadeh, Rashid, & Cinar, 2018a; Hajizadeh et al., 2018b). The recursive system identification technique provides a time-varying stable state-space model and updates its parameters when new CGM data are received (5 min sampling time). By integrating the time-varying linear model with a physiological compartment dynamics (Hajizadeh et al., 2018a), the dynamic model of the system can be written as:

$$\begin{aligned} x_k &= A_k x_{k-1} + B_k u_k + \omega_k \\ y_k &= C_k x_k + D_k u_k + \nu_k \end{aligned} \tag{1}$$

where $x_k \in \mathbb{R}^{n_x}$, $y_k \in \mathbb{R}^{n_y}$, $u_k \in \mathbb{R}^{n_u}$, $\omega_k \in \mathbb{R}^{n_x}$, and $\nu_k \in \mathbb{R}^{n_y}$ represent state variables, the model output, input variables, zero-mean Gaussian random process and measurement noise vectors, respectively. The time-varying matrices $A_k \in \mathbb{R}^{(n_x \times n_x)}$, $B_k \in \mathbb{R}^{(n_x \times n_u)}$, $C_k \in \mathbb{R}^{(n_y \times n_x)}$, $D_k \in \mathbb{R}^{(n_y \times n_u)}$ are also the dynamic state, input, output, and direct feed-through matrices which are updated at each sampling time. In Eq. (1), CGM is the output variable, injected insulin information (both basal and bolus insulin infusion), estimation of the meal effect, and physiological variables are inputs that indicate physical activity ($u_k = [Ins_k, Meal_k, MET_k]$). Metabolic equivalent of task (MET) value denotes energy expenditure and represents the metabolic equivalent of the activity. The amount of insulin in the bloodstream, which is called plasma insulin concentration (PIC), is one of the state variables of the state-space model (1). Due to medical considerations,the PIC constraints are defined in the objective function to guarantee that a safe amount of insulin circulating in the bloodstream. Using Kalman filter representation, the identified glycemic model for use in adaptive MPC can be represented in the following state-space form:

$$\begin{aligned} \hat{x}_{k|k-1} &= A_k \hat{x}_{k-1|k-1} + B_k u_k \\ \hat{x}_{k|k} &= \hat{x}_{k|k-1} + K_k \tilde{y}_{k|k} \\ y_k &= C_k \hat{x}_{k|k-1} + D_k u_k + \tilde{y}_{k|k} \end{aligned} \tag{2}$$

where vector $\hat{x}_{k|k} \in \mathbb{R}^{(n_x \times n_x)}$ is the *a posteriori* estimated state variables and $K_k \in \mathbb{R}^{(n_x \times n_u)}$ denotes the optimal Kalman filter gain, contributing the correction term added to the estimated state variables. $\tilde{y}_{k|k} \in \mathbb{R}^{n_y}$ is the error estimation of the output y_k. The time-varying estimation of A_k, B_k, C_k, D_k, and Kalman gain K_k are obtained by solving least squares optimization problem as detailed in Appendix A and Appendix B.

2.2. Variable prediction using dynamic latent variable model

In the state-space model (1), the injected insulin is the manipulated variable. Estimates of the meal effect, physiological variables, and MET value are also exogenous input disturbances affecting the underlying system. The estimated linear dynamics of insulin-glucose variations is utilized to forecast the future evolution of the state variables in the formulation of MPC. Since the identified model cannot precisely forecast the CGM GC over long prediction horizons, the performance of the closed-loop system has potential to deteriorate. In fully automated insulin delivery systems, no manual information about disturbances (meals, physical activities) is provided, and regulating the GC becomes more challenging. In such cases, historical data can be processed to further improve the robustness of the system by estimating the future progression of the CGM and also by predicting MET values and meal effects as exogenous disturbances of the system (1).

As the first objective of this work, unknown disturbances are forecasted by using data analytics and ML with historical data. The past data used in the learning approach are: i) CGM measurements, ii) injected insulin data, iii) estimates of meal effect, iv) physiological variables indicating physical activity, v) PIC estimates, vi) the first and second derivatives of CGM data (computed by fitting a second order polynomial to the last few CGM values and calculating numerical derivatives) to detect the effect of disturbances such as meal and exercise, and vi) unmeasured sensor noise. Assume that N days of previously sampled data are available (Fig. 2). It is desired to adaptively estimate the current evolving pattern with the past measurements to obtain the most similar scenarios for the prediction of unknown disturbances with meal and exercise times and characteristics varying every day, as illustrated in Fig. 3. The first step for determining the most likely and worst-case scenarios for unannounced disturbances is to categorize unknown disturbances based on their similarities. DrLVR (Zhu et al., 2020) is utilized to forecast the future time-series of the feature variables

$$T_f = \left[\widehat{PIC}, MET, CGM, C\dot{G}M, C\ddot{G}M, Meal, Ins, d\right].$$

where $CGM = \left[CGM_1, \ldots, CGM_{NL_s}\right]^T$ is the vector of N days historical CGM data with L_s samples per day. Likewise, $C\dot{G}M$, $C\ddot{G}M$, *d, Meal, Ins*, $\widehat{PIC}$, and *MET* represent the vector of the first and second derivatives of CGM values, estimated uncertainties, the effect of meal, the amount of injected insulin, the estimation of PIC, and the MET value, respectively. Qualitative trend analysis of CGM inferred by the sign of the first and

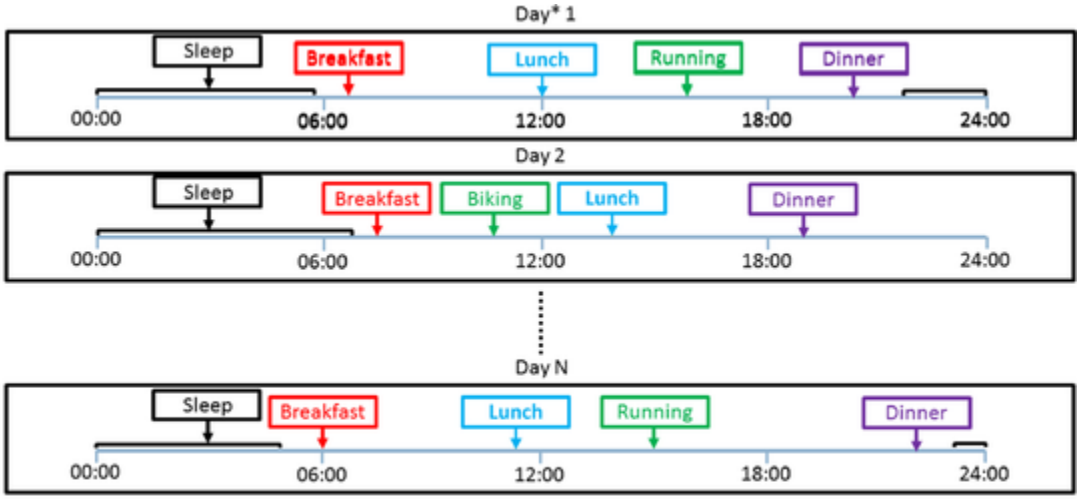

Fig. 2. Batch representation of the historical data.

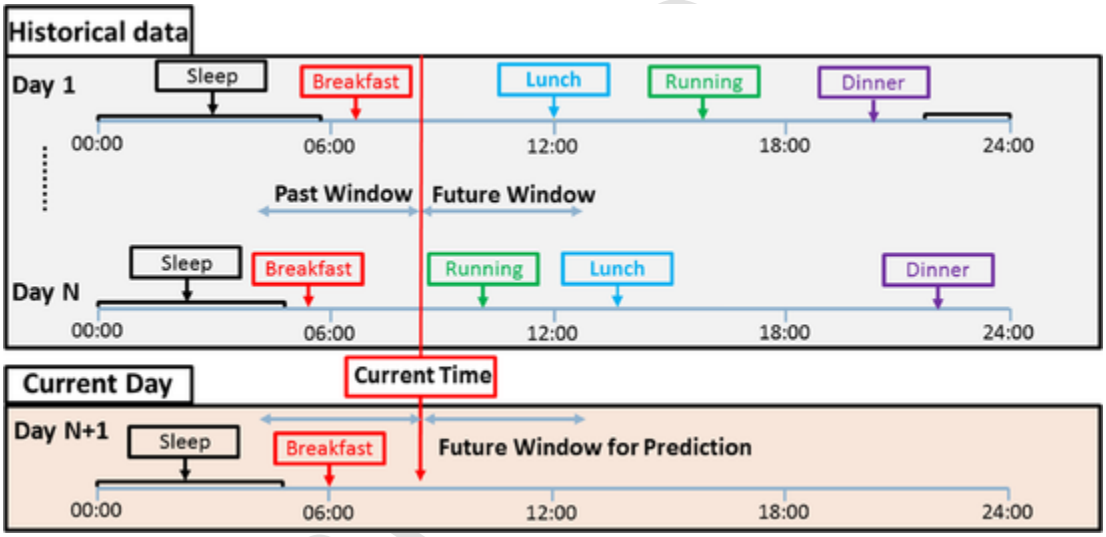

Fig. 3. Disturbance prediction from historical data.

second derivatives of CGM convey useful information about the future variation of CGM (Samadi et al., 2018; 2017) and consequently, the potential occurrence of hypoglycemia ($GC < 70\,mg/dL$) or hyperglycemia ($GC > 180\,mg/dL$). Hence, the first and second derivatives of CGM are included in the matrix of T_f.

Although DrLVR is a supervised method to model output variables from input data, it can also be applied for unsupervised pattern estimation of time-series data. In DrLVR, Markov parameters of an inner Vector Auto-regressive (VAR) model is extracted to describe the output score $u_s \in \mathbb{R}^{\mathcal{N}}$ from the past $s \geq 1$ input score vectors as

$$\hat{u}_s = \sum_{i=0}^{s} \alpha_i t_{s-i} \tag{3}$$

Based on the DrLVR algorithm proposed by Zhu et al. (2020), the first s steps-ahead samples of the output variables is not predicted and the algorithm only calculates sample $s+1$ of the output variable. For simplicity in notation let $\mathcal{X} = [\mathcal{X}^{(1)}, \ldots, \mathcal{X}^{(8)}] = [\widehat{PIC}, \ldots, d]$. To obtain a sequence of future prediction, we define the lagged matrices of input and output variables, $\mathcal{X}_L \in \mathbb{R}^{(\mathcal{N}+s\times\mathcal{M}_p)}$ and $\mathcal{Y}_L \in \mathbb{R}^{(\mathcal{N}+s\times\mathcal{M}_f)}$, as:

$$\mathcal{X}_L = \left[\mathcal{X}^{(1)}_{m_p}, \ldots, \mathcal{X}^{(8)}_{m_p}\right] = \left[\mathcal{X}_{L,1}, \ldots, \mathcal{X}_{L,\mathcal{N}+s}\right]^T$$
$$\mathcal{Y}_L = \left[\mathcal{Y}^{(1)}_{m_f}, \ldots, \mathcal{Y}^{(8)}_{m_f}\right] = \left[\mathcal{Y}_{L,1}, \ldots, \mathcal{Y}_{L,\mathcal{N}+s}\right]^T$$

$$\mathcal{X}^{(j)}_{m_p} = \begin{bmatrix} \mathcal{X}^{(j)}_{1} & \cdots & \mathcal{X}^{(j)}_{m_p} \\ \mathcal{X}^{(j)}_{2} & \cdots & \mathcal{X}^{(j)}_{m_p+1} \\ \vdots & \ddots & \vdots \\ \mathcal{X}^{(j)}_{\mathcal{N}+s} & \cdots & \mathcal{X}^{(j)}_{\mathcal{N}+s+m_p-1} \end{bmatrix}$$

$$\mathcal{Y}^{(j)}_{m_f} = \begin{bmatrix} \mathcal{X}^{(j)}_{m_p-s} & \mathcal{X}^{(j)}_{m_p-s+1} & \cdots & \mathcal{X}^{(j)}_{m_p+m_f-s} \\ \mathcal{X}^{(j)}_{m_p-s+1} & \mathcal{X}^{(j)}_{m_p-s+2} & \cdots & \mathcal{X}^{(j)}_{m_p+m_f-s+1} \\ \vdots & \vdots & \ddots & \vdots \\ \mathcal{X}^{(j)}_{NL_s-m_f} & \mathcal{X}^{(j)}_{NL_s-m_f+1} & \cdots & \mathcal{X}^{(j)}_{NL_s} \end{bmatrix}.$$

where $\mathcal{N} = NL_s - m_p - m_f + s - 1$, $\mathcal{M}_f = 8m_f$, and $\mathcal{M}_p = 8m_p$. m_p is also the number of past samples used to predict time-series variations of the feature variables, $\mathcal{X}^j, j = 1, \ldots, 8$ and $m_f < m_p$ is the prediction horizon. Define the s-lagged dynamic-order matrices $X_i \in \mathbb{R}^{(\mathcal{N}\times\mathcal{M}_p)}$,

$Y_s \in \mathbb{R}^{(\mathcal{N}\times\mathcal{M}_f)}$, as given by

$$X_i = \left[\mathcal{X}_{L,i+1}, \ldots, \mathcal{X}_{L,i+\mathcal{N}}\right]^T,\ i = 0, \ldots, s$$
$$Y_s = \left[\mathcal{Y}_{L,s+1}, \ldots, \mathcal{Y}_{L,s+\mathcal{N}}\right]^T \tag{4}$$

The formulation of DrLVR is to find autoregressive Markov parameters $\beta_j \in \mathbb{R}^{s+1}$, weight vectors $w_j \in \mathbb{R}^{\mathcal{M}_p}$, and $q_j \in \mathbb{R}^{\mathcal{M}_f}$ for each latent variable $j = 1, \ldots, l$ that maximize the following constrained objective function

$$w^*, q^*, \beta^* = \underset{w,q,\beta}{argmax}\ q^T Y_s^T T_S \beta - \frac{\gamma}{2}\|w\|^2$$
$$s.t \quad \{\|\beta\| = 1,\ \|q\| = 1,\ \|T_s\beta\| = 1\} \tag{5}$$

where $T_s \in \mathbb{R}^{s+1}$ denote the vector of input score. The batch-wise procedure of DrLVR algorithm is given in Appendix C. The decomposed matrices $\mathcal{X}_L$ and $\mathcal{Y}_L$ are expressed by using extracted score matrices $T \in \mathbb{R}^{(\mathcal{N}+s)\times l}$, $\hat{U}_s \in \mathbb{R}^{\mathcal{N}\times l}$ and loading matrices $\mathcal{P} \in \mathbb{R}^{\mathcal{M}_p \times l}$ and $\mathcal{C} \in \mathbb{R}^{\mathcal{M}_f \times l}$ as

$$\mathcal{X}_L = \sum_{i=1}^{l} t^{(i)} p^{(i)T} + E = \mathcal{T}\mathcal{P}^T + E$$
$$Y_s = \sum_{i=1}^{l} \hat{u}_s^{(i)} c^{(i)T} + F = \hat{U}_s \mathcal{C}^T + F \tag{6}$$

where $E \in \mathbb{R}^{(\mathcal{N}+s)\times\mathcal{M}_p}$ and $F \in \mathbb{R}^{(\mathcal{N}+s)\times\mathcal{M}_f}$ represent residual matrices carrying static correlation between variables $\mathcal{X}_L$ and Y_s. At each sampling time k, the estimation of the new input matrix $\mathcal{X}_{L,new}$ can be calculated as

$$\hat{Y}_s = \hat{U}_s \mathcal{C}^T \tag{7}$$

where $\hat{U}_s$ is calculated from $\mathcal{T}_{new} = \mathcal{X}_{L,new}\mathcal{W}\left(\mathcal{P}^T\mathcal{W}\right)^{-1}$ and Eq. (3). Since scores, loadings, and the matrices of input and output data are being updated at each sampling time k, DrLVR algorithm needs to be executed repeatedly. As a proper choice for initialization, vectors $\beta_k^{(i)}$ and $u_{s,k}^i, i = 1, \ldots, l$ can be initialized with their values calculated from the previous time instance. Eq. (7) calculates time-series prediction of output variables over the horizon $m_f - s$. The insulin-glucose dynamics of the body show daily patterns that can be used to enhance the accuracy and robustness of the prediction. In order to take into account the occurrence of extreme disturbances, $\pm$ 1.645 standard deviations, encompassing 5–95 percentile of the interval of times-series samples collected from the past N_s days are calculated as upper and lower bounds (envelops) of the predicted feature variables predicted from DrLVR. Considering these predictions in the objective function improves the robustness of the controller against worst-case scenarios. Fig.(4) demonstrates the prediction scheme over the prediction horizon $m_f - s$.

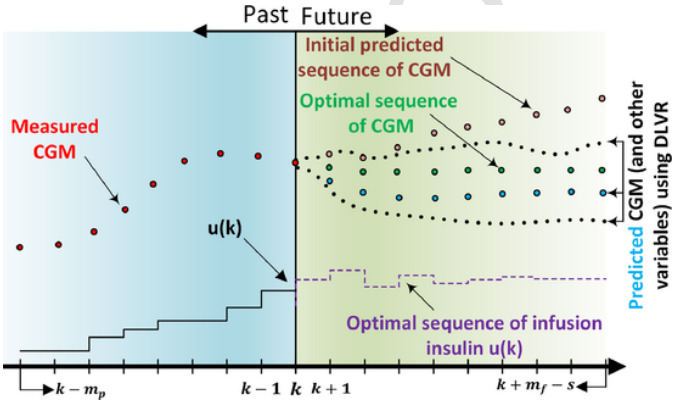

Fig. 4. The prediction scheme from historical data using DrLVR and its incorporation with MPC.

2.3. Adaptive learning model predictive control

The PIC-cognizant AL-MPC calculates the optimal insulin injection rate by employing adaptive weights that modify the penalty weighting matrices in the MPC objective function. It calculates the optimal insulin injection rate over a finite horizon by using the recursively identified subspace-based dynamic models and three different predictions obtained for the unknown process disturbances by solving the following quadratic programming problem at each sampling time k

$$\left\{\mathbf{z}_{i,j}^*, \mathbf{m}_i^*\right\}_{i=0}^{m_f-s} :=$$
$$\underset{\substack{\mathbf{z}_j \in \mathcal{Z} \\ \mathbf{m} \in \mathcal{M}}}{\operatorname{argmin}}\ \mathcal{J}_{k,m_f-s}\left(\mathcal{Q}_{j,k}, P_k, \mathcal{R}_k, \left\{\mathbf{m}_i\right\}_{i=0}^{m_f-s}, \left\{\mathbf{z}_{j,i}\right\}_{i=0}^{m_f-s}\right)$$

$$\text{s.t.} \begin{cases} \mathbf{z}_{j,i+1} = A_k \mathbf{z}_{j,i} + B_k \mathbf{m}_i + d_{j,i} \\ \mathbf{q}_{j,i} = C_k \mathbf{z}_{j,i} + D_k \mathbf{m}_i \\ \mathbf{z}_{j,0} = \hat{x}_{j,k} \\ \mathbf{m}_{j,i}^{min} \le \mathbf{m}_i \le \mathbf{m}_{j,i}^{max} \\ \mathbf{z}_{j,i}^{PIC,min} \le \mathbf{z}_{j,i}^{PIC} \le \mathbf{z}_{j,i}^{PIC,max} \\ \mathbf{e}_{j,i}^{PIC} = \mathbf{z}_{j,i}^{PIC} - \mathbf{z}_{j,i}^{PIC,des} \\ \mathbf{z}_{j,i}^{PIC,max} = \left(\beta_{m,k} + \beta_f\right) \times \left(a_{j,i}^{max} \times \mathbf{q}_{j,i} + b_{j,i}^{max}\right) \\ \mathbf{z}_{j,i}^{PIC,min} = \left(\beta_{m,k} + \beta_f\right) \times \left(a_{j,i}^{min} \times \mathbf{q}_{j,i} + b_{j,i}^{min}\right) \\ \mathbf{z}_{j,i}^{PIC,des} = \left(\beta_{m,k} + \beta_f\right) \times \left(a_{j,i}^{des} \times \mathbf{q}_{j,i} + b_{j,i}^{des}\right) \end{cases} \tag{8}$$

incorporated with the objective function

$$\mathcal{J}_{k,m_f-s} := \sum_{i=0}^{m_f-s} \sum_{j=1}^{3} \left(\mathbf{q}_{j,i} - \mathbf{r}_{j,i}\right) \mathcal{Q}_{j,k} \left(\mathbf{q}_{j,i} - \mathbf{r}_{j,i}\right)$$
$$+ \left(\mathbf{m}_i - \mathbf{m}_{basal_i}\right) \mathcal{R}_k \left(\mathbf{m}_i - \mathbf{m}_{basal_i}\right) + \mathbf{e}_{j,i}^{PIC} P_k \mathbf{e}_{j,i}^{PIC} \tag{9}$$

where $\mathbf{z}_{j,k} \in \mathbb{R}^{n_x}$ and $\mathbf{q}_{j,k} \in \mathbb{R}$ represent the estimated state variables and the output of the model, respectively. For the prediction/control horizon $m_f - s$, $\mathbf{m}_i \in \mathbb{R}$ represents the constrained input variable, which takes values in a nonempty convex set $\mathcal{M} := \left\{\mathbf{m}_k \in \mathbb{R} : \mathbf{m}_{j,k}^{\min} \le \mathbf{m}_k \le \mathbf{m}_{j,k}^{\max}\right\}$ with $\mathbf{m}_{j,k}^{\min} \in \mathbb{R}$ and $\mathbf{m}_{j,k}^{\max} \in \mathbb{R}$ denote the lower and upper limits on the manipulated variable, respectively. $r_{j,k}$ is the target set-point, and $\mathbf{m}_{basal_k}$ is the patient-specified rate of basal insulin. The nonempty convex set $\mathcal{Z}$ with $\mathcal{Z} := \left\{\mathbf{z}_{j,k} \in \mathbb{R}^{n_x} : \mathbf{z}_{j,k}^{\min} \le \mathbf{z}_k \le \mathbf{z}_{j,k}^{\max}\right\}$, $\mathbf{z}_{j,k}^{\min} \in \mathbb{R}^{n_x}$ and $\mathbf{z}_{j,k}^{\max} \in \mathbb{R}^{n_x}$ represent the lower and upper bounds on state variables, respectively, with one of the state variables as the estimated PIC ($\mathbf{z}_{j,k}^{PIC}$) that is constrained by the PIC limits ($\mathbf{z}_{j,k}^{PIC,max}$, $\mathbf{z}_{j,k}^{PIC,min}$, and $\mathbf{z}_{j,k}^{PIC,des}$) where the $\mathbf{z}_{j,k}^{PIC,des}$ is the desired PIC value. The number of state variables in the integrated glycemic model (2) is n_x, $\hat{x}_{j,k}$ provides an initialization of the vector of state variables, $\mathcal{Q}_{j,k} \ge 0$ is a positive semi-definite symmetric matrix utilized to penalize the deviations of the outputs from their desired set-point, and $\mathcal{R}_k$ and P_k are strictly positive definite symmetric matrix to penalize manipulated variables and the PIC errors, respectively. At each iteration, the quadratic programming problem described by (8) is solved, and $u_k := \mathbf{m}_0$ which is the optimal solution implemented to inject insulin over the current control horizon with the MPC computation repeated at next sampling time using new CGM data, energy expenditure, updated state variables, and newly computed penalty weights of the objective function.

3. Simulation results

The simulator mGIPsim is utilized to assess the performance of AL-MPC (Rashid et al., 2019). A scenario for a period of 30 days with varying times and amounts of daily meals and physical activity durations and intensities are used. Tables 1 and 2 provide the ranges in

Table 1
Meal scenario for 30-days CL experiment using mGIPsim.

Meal	Range for values	
	Time	Amount (g)
Breakfast	[06: 00, 07: 00]	[40, 60]
Lunch	[12: 00, 13: 00]	[40, 60]
Dinner	[18: 00, 19: 00]	[40, 60]

Table 2
Exercise scenario for 30-days CL experiment using mGIPsim.

Exercise	Range for values		
	Time	Duration (min)	Power
Bicycling	[10: 00, 11: 00]	[30, 60]	[50, 90]
Bicycling	[16: 00, 17: 00]	[30, 60]	[50, 90]

mealtimes and its amounts, and exercise times, durations, and intensities. Daily values are randomly selected from these ranges. The controller set-point is set to a GC of 110 *mg/dL* except during exercise when it takes the value of 160 *mg/dL*. Aerobic activities with a stationary bicycle are considered for testing the mAP. The meal and physical activity information are not manually entered into the mAP and are predicted only from "sensor" information generated by mGIPsim. The mAP controller is a fully automated system, rather than a hybrid closed-loop AP, designed to regulate the GC in the presence of significant unknown disturbances such as unannounced meals and physical activities occurring at varying times and having characteristics that change randomly. The energy expenditure values, expressed as MET variations, are computed by mGIPsim and utilized as an input variable. The calculated EE values summarize the physiological signal variations caused by physical activities.

Table 3 summarizes the quantitative evaluation of the closed-loop (CL) operation based on the proposed algorithms and results are compared with regular MPC without learning and with two different learning techniques used for estimating significant disturbances and the future evolution of controlled variable. The simulation results are also repeated for dynamic PCA (DiPCA) (Dong & Qin, 2018) with kNN (DiPCA-kNN) and k-means hyperspherical clustering techniques for comparison. These simulation studies are intended to illustrate that the mAP incorporated with evolution and DrLVR learning method is robust and reliable in learning and recognizing the patients' habits and daily activities. The mean percentage of time spent in the target ranges of [70,140] mg/dL and [70,180] mg/dL are 59.2% and 84.4% for all subjects. No hypoglycemic event was detected as the GC never dropped below 70 *mg/dL*. The forecasted hypoglycemic episodes inform the subject to consume rescue carbohydrates about 20 minutes before the potential hypoglycemic event. The mean of the minimum and maximum observed GC values over all clinical experiments during the simulation are 80.2 and 235.1 *mg/dL*, respectively. In general, the simulation results show that the proposed mAP with AL-MPC is capable of controlling GC efficiently in the presence of significant unannounced disturbances. Regardless of the changing timing and amounts of carbohydrates and physical activity specifications, the proposed mAP can mitigate the effects of meals and exercise, prevent severe hypoglycemic events, and decrease the number and duration of hyperglycemic events.

4. Discussion

CL simulation results for all subjects for the last day of simulations are summarized in Fig. 5. As can be seen, in comparison to the adap-

Table 3
CL simulation results for AL-MPC whole days.

Subject	Percent of time in range					GC Statistics			
	< 70	[70, 140]	[70, 180]	> 180	> 250	Mean	SD	Min	Max
S1	0	51.7	81.3	17.7	0	143.9	33.1	92.2	236.6
S2	0	60.2	86.8	13.11	0	138.0	32.0	72.8	226.5
S3	0	65.1	87.2	12.8	0	133.7	32.0	85.6	225.7
S4	0	65.2	89.7	10.3	0	133.2	31.5	73.5	230.5
S5	0	68.5	90.9	9.1	0	129.1	30.8	70.4	225.7
S6	0	60	93.8	6.2	0	135.7	25.4	76.9	219.4
S7	0	66.6	88.2	11.8	0	132.9	31.5	79.6	234.5
S8	0	64.8	87.8	12.2	0	133.4	31.4	86.2	232.1
S9	0	46.5	73.7	26.3	0.4	153.2	39.0	83.6	264.1
S10	0	67.1	86.7	13.3	0	133.1	33.3	72.9	237.2
S11	0	57.8	86.4	13.6	0	138.5	32.8	73.2	233.9
S12	0	58.2	84.5	15.5	0	140.4	32.7	78.7	232.6
S13	0	50.4	77.7	22.3	0.3	148.6	36.3	81.7	271.7
S14	0	58.7	84.6	15.4	0	138.9	34.7	74.1	240.6
S15	0	60.6	86.6	13.4	0	139.9	29.6	92.3	228.5
S16	0	69.9	92.6	7.4	0	130.5	27.1	78.8	213.3
S17	0	60.8	81.9	18.1	0	138.3	36.1	72.8	237
S18	0	46.5	64.8	35.2	0.2	157.1	43.9	88.3	253.8
S19	0	57.4	91.9	8.1	0	138.1	26.6	90.6	217.7
S20	0	49.4	72.4	27.6	0	150.3	38.7	84.0	240.8
Average(AL-MPC)	**0**	**59.2**	**84.4**	**15.5**	**0.04**	**139.3**	**32.9**	**80.2**	**235.1**
Average(k-means) Hajizadeh et al. (2020 (in press)	**0**	**55.1**	**78.2**	**21.8**	**0.1**	**145.3**	**36.2**	**82.0**	**244.0**
Average(DiPCA- k-NN)	**0.0017**	**59.8**	**83.9**	**16.0**	**0.05**	**139.3**	**33.4**	**79.4**	**236.4**
Average(A-MPC)	**0.0035**	**59.4**	**82.5**	**17.5**	**0.04**	**140.5**	**34.2**	**80.8**	**232.0**

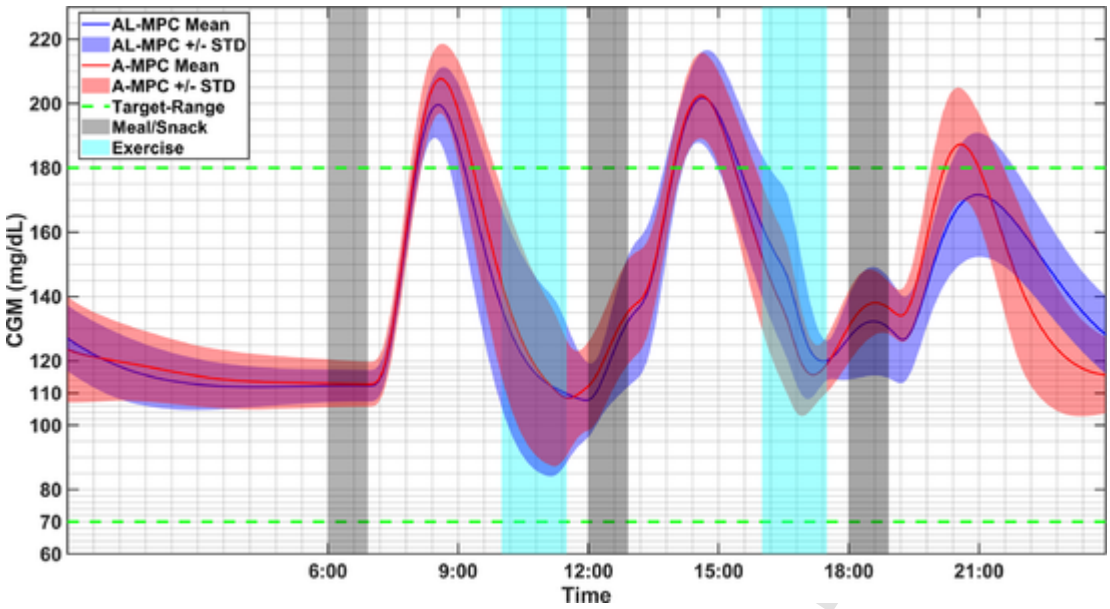

Fig. 5. CL results for all subjects on day 30.

tive mAP with an A-MPC that lacks learning features, the mAP with AL-MPC is able to keep the GC values in a higher range during physical activity. Hypoglycemia prevention is performed by considering a higher controller set-point prior to observing the effect of physical activity, which is detected by forecasting the MET values. A comparison of the averages reported in Tables 3 and 4 indicates that the AL-MPC is well-adapted to glucose dynamics as it can better maintain the GC within the desired range without utilizing excessive insulin. By the long-window prediction horizon, AL-MPC can take into account the time-delay prandial GC response and also GC drop during physical activity.

Table 4
The number of predicted hypoglycemic events (# PH) and inhibitions by rescue carbohydrates for the whole simulation period (30 days) and the average of total daily injected insulin (TDI) (U) with AL-MPC (results for A-MPC without learning in parentheses).

Subject	# ph	TDI (U)
S1	**68** (110)	**39.5** (41.7)
S2	**109** (122)	**38.6** (39.3)
S3	**83** (109)	**33.4** (34.1)
S4	**90** (97)	**34.0** (34.2)
S5	**123** (126)	**29.4** (29.1)
S6	**82** (106)	**41.5** (42.7)
S7	**66** (73)	**42.0** (42.0)
S8	**79** (104)	**31.3** (32.1)
S9	**58** (55)	**63.3** (62.7)
S10	**73** (81)	**28.8** (28.5)
S11	**86** (90)	**32.8** (31.6)
S12	**75** (101)	**26.6** (27.5)
S13	**29** (28)	**49.4** (47.8)
S14	**114** (113)	**30.1** (29.3)
S15	**30** (57)	**44.3** (45.7)
S16	**100** (124)	**44.5** (45.0)
S17	**114** (120)	**27.0** (27.3)
S18	**19** (55)	**50.6** (53.5)
S19	**75** (106)	**46.6** (48.5)
S20	**30** (58)	**45.7** (47.1)
Average	**75** (92)	**39.02** (39.5)

Thirty days of CL simulation results for a randomly chosen subject is displayed in Fig. 6. It illustrates that mAP integrated with learning feature enhances the reliability and safety of the insulin delivery system, especially after carbohydrate consumption and during physical activity. In general, the AL-mAP algorithm can regulate the CGM with the minimum need for hypoglycemia considerations. Table 4 shows the average reduction in predicted hypoglycemic episodes necessitating rescue carbohydrates from 92 to 75 and total daily injected insulin from 39.5 to 39.0. The lower number of hypoglycemic events indicates that the controller action (insulin doses) calculated is safer, and the controller is more conservative compared to mAP without learning features. A reduction in the value of ph and an increase in the duration of normal glycemic periods (GC 70–180 *mg/dL*) shows that the controller becomes more reliable in keeping the GC closer to the set-point with a minimum risk of hyper- and hypoglycemic events.

5. Conclusions

An adaptive MPC with learning capability is proposed for controlling uncertain nonlinear processes with time-varying characteristics. As a case study, the glucose-insulin dynamics of the human body is utilized to test the efficiency and effectiveness of the AL-MPC algorithm. The proposed control framework incorporates uncertainty quantification, disturbance prediction, adaptive learning, and recursive subspace identification. DrLVR technique can detect patterns in historical data to improve the performance of MPC. Simulation results show that the learning technique employed in the formulation of the MPC controller can significantly improve the regulation of glucose concentrations without causing undesired outcomes of very high or very low glucose levels.

Declaration of Competing Interest

The authors declare that they have no known competing financial interests or personal relationships that could have appeared to influence the work reported in this paper.

Acknowledgements

This work is supported by the National Institute of Diabetes and Digestive and Kidney Diseases grants DP3 DK101075-01 and DP3

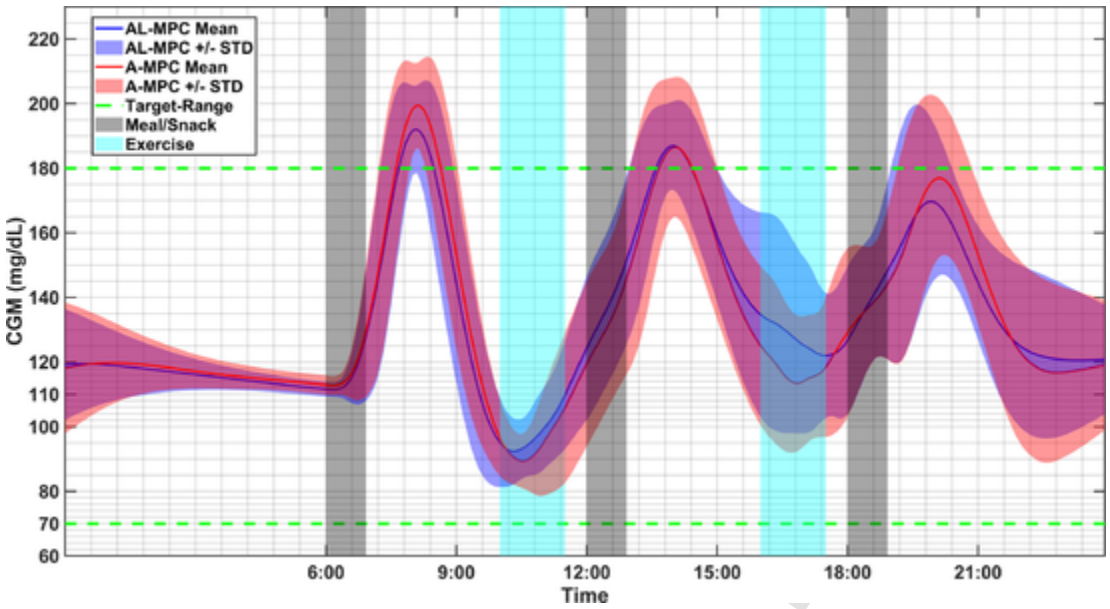

Fig. 6. CL results for one select subject during whole simulation.

DK101077-01 and JDRF grants 17-2013-472, and 2-SRA-2017-506-M-B made possible through collaboration between JDRF and The Leona M. and Harry B. Helmsley Charitable Trust.

Appendix A. - Recursive subspace identification algorithm

In what follows, the summarized description of PBSID proposed by Houtzager, van Wingerden, and Verhaegen (2011) is briefly explained. The objective is to identify the controllable and observable part of single input single output ($n_u = 1, n_y = 1$) dynamic system (1) and also calculate the optimal Kalman gain K. Let define the output lagged vectors, $\bar{y}_{k-m_p} \in \mathbb{R}^{m_p}$ and multi-step ahead vectors $\bar{y}_{k+m_f} \in \mathbb{R}^{m_f}$ as

$$\begin{aligned} \bar{y}_{k-m_p} &= \left[y_{k-m_p}, y_{k-m_p+1}, \cdots, y_{k-1}\right]^T \\ \bar{y}_{k+m_f} &= \left[y_k, y_{k+1}, \cdots, y_{k+m_f-1}\right]^T \end{aligned} \tag{A.1}$$

similarly, the corresponding input lagged vectors, $\bar{u}_{k-m_p} \in \mathbb{R}^{m_p}$ and multi-step ahead vectors $\bar{u}_{k+m_f} \in \mathbb{R}^{m_f}$ can be defined. Generating the past estimated variables $\hat{x}_{j|j-1}, j = k, \ldots, k-m_p$ and the future output variables $\bar{y}_{k+m_f}$ from state observer Eq. (2) gives

$$\begin{aligned} \hat{x}_{k|k-1} &= \widetilde{A}^{m_p}\hat{x}_{k-m_p|k-m_p} + \widetilde{\mathscr{L}}\bar{u}_{k-m_p} + \widetilde{\mathscr{K}}\bar{y}_{k-m_p|k-m_p} \\ \bar{y}_{k+m_f} &= \widetilde{\Gamma}\hat{x}_{k|k} + \widetilde{\mathscr{G}}\bar{y}_{k+m_f} + \left(I - \widetilde{\mathscr{K}}\right)\bar{y}_{k+m_f|k+m_f} \\ &\quad + \bar{\bar{y}}_{k+m_f|k+m_f} \end{aligned} \tag{A.2}$$

where $\widetilde{A} = A - KC$ and $\widetilde{B} = B - KD$ and $\bar{\bar{y}}_{k+m_f|k+m_f} \in \mathbb{R}^{m_f}$ is the lagged vector of estimation error defined similar to Eq. (A.1). The extended controlability matrices $\widetilde{\mathscr{L}} \in \mathbb{R}^{n_x \times m_p}$ and $\widetilde{\mathscr{K}} \in \mathbb{R}^{n_x \times m_p}$ and the extended observability matrix $\widetilde{\Gamma} \in \mathbb{R}^{m_f \times n_x}$ are defined by

$$\begin{aligned} \widetilde{\mathscr{L}} &= \left[\widetilde{A}^{p-1}\widetilde{B}, \widetilde{A}^{p-2}\widetilde{B}, \ldots, \widetilde{A}\widetilde{B}, \widetilde{B}\right] \\ \widetilde{\mathscr{K}} &= \left[\widetilde{A}^{p-1}K, \widetilde{A}^{p-2}K, \ldots, \widetilde{A}K, K\right] \\ \widetilde{\Gamma} &= \left[C, C\widetilde{A}, \ldots, C\widetilde{A}^{m_f-1}\right]^T \end{aligned} \tag{A.3}$$

The columns of lower rectangular matrices $\widetilde{\mathscr{G}} \in \mathbb{R}^{m_f \times m_f}$, and $\widetilde{\mathscr{K}} \in \mathbb{R}^{m_f \times m_f}$ are given as

$$\begin{aligned} \widetilde{\mathscr{G}}_i &= \left[\underbrace{0, \ldots, 0}_{i-1}, D, \underbrace{C\widetilde{B}, C\widetilde{A}\widetilde{B}, C\widetilde{A}^{m_f-j}\widetilde{B}}_{f-i-1}\right]^T \\ \widetilde{\mathscr{K}}_i &= \left[\underbrace{0, \ldots, 0}_{i-1}, I_{n_y}, \underbrace{-CK, -C\widetilde{A}K, -C\widetilde{A}^{m_f-j}K}_{f-i-1}\right]^T. \end{aligned} \tag{A.4}$$

As stated in Houtzager et al. (2011), we assume that the asymptotic stable matrix $\widetilde{A}$ satisfies nilpotency condition assumption (Chiuso & Picci, 2005), where $\widetilde{A}^j \approx 0, j \geqslant n_p$. Therefore, the first equation of (A.2) can be rearranged to

$$\hat{x}_{k|k-1} \approx \widetilde{\mathscr{L}}\bar{u}_{k-m_p} + \widetilde{\mathscr{K}}\bar{y}_{k-m_p|k-m_p} \tag{A.5}$$

The formulation of the PBSID is established through employing a vector autoregressive with exogenous input (VARX) model for one step ahead prediction of $\hat{y}_{k|k-1}$ as

$$\hat{y}_{k|k-1} = \sum_{i=0}^{m_p}\theta^{(u)}_{k-i}u_{k-i} + \sum_{i=1}^{m_p}\theta^{(y)}_{k-i}y_{k-i} \tag{A.6}$$

where the VARX model parameters to be estimated are

$$\Theta_k \triangleq \left[\theta^{(u)}_k, \ldots, \theta^{(u)}_{k-m_p}, \theta^{(y)}_{k-1}, \ldots, \theta^{(y)}_{k-m_p}\right] \tag{A.7}$$

as it has been proven in Chiuso and Picci (2005), the following equations hold for the unknown parameters of the vector Θ_k as detailed in

$$\begin{aligned} \theta^{(u)}_{k-j} &= \begin{cases} D, & if \\ C\widetilde{A}^{m_p-j-1}\widetilde{B}, & if \quad j \end{cases} \\ \theta^{(y)}_{k-j} &= C\widetilde{A}^{m_p-j}\widetilde{K} \end{aligned} \tag{A.8}$$

As shown in Houtzager et al. (2011), two multiplied matrices $\widetilde{\Gamma} \times \widetilde{\mathscr{L}}$ and $\widetilde{\Gamma} \times \widetilde{\mathscr{K}}$ is calculated from the estimated Markov parameters (A.7) as:

$$\widetilde{\Gamma}\widetilde{\mathscr{L}} = \begin{bmatrix} \theta_k^{(u)} & \theta_{k-1}^{(u)} & \cdots & \theta_{k-f}^{(u)} & \cdots & \theta_{k-m_p+1}^{(u)} \\ 0 & \theta_k^{(u)} & \cdots & \theta_{k-f+1}^{(u)} & \cdots & \theta_{k-m_p+2}^{(u)} \\ \vdots & \ddots & \ddots & \vdots & \ddots & \vdots \\ 0 & \cdots & 0 & \theta_k^{(u)} & \cdots & \theta_{k-m_p+m_f}^{(u)} \end{bmatrix} \tag{A.9}$$

similarly, $\widetilde{\Gamma} \times \widetilde{\mathscr{K}}$ can be calculated from the lagged matrix stacked with parameters $\theta_k^{(y)}, \ldots, \theta_{k-m_p+1}^{(y)}$. As an option, Singular Value Decomposition(SVD) can be applied to calculate $\hat{x}_{k|k-1}$ in Eq. (A.5). In recursive identification, modifying SVD factorization can be rather complicated and inefficient. Hence, most recursive system identification extract approximate low-rank, (A.5) as

$$\hat{x}_{k|k-1} = S_k W_k \left(\widetilde{\Gamma}\widetilde{\mathscr{L}}\bar{u}_{k-m_p} + \widetilde{\Gamma}\widetilde{\mathscr{K}}\bar{y}_{k-m_p|k-m_p} \right) \tag{A.10}$$

where $S_k \in \mathbb{R}^{(n_x \times m_f)}$ is the selection matrix and it can be estimated using the gradient approach suggested in Oku and Kimura (2002). Let $\phi_k = \left[\hat{x}_k^T, \hat{u}_k^T\right]^T$ and $\psi_k = \left[\hat{x}_{k-1}^T, \hat{u}_{k-1}^T, \tilde{y}_{k-1|k-1}^T\right]^T$ be the basis matrices and $\Theta_k^{(y)} = \left[C_k, D_k\right]^T$, $\Theta_k^{(x)} = \left[A_k B_k K_k\right]^T$ be the state-space parameters matrices. Then, at each time instance k two least squares problems for the estimation of A_k, B_k, C_k, D_k, and K_k need to be solved over the past batch of the input-output data.

$$\begin{aligned} \Theta_{k,opt}^{(y)} &:= \underset{\Theta_k^{(y)}}{argmin} \sum_{i=k-m_p}^{k} \left\| \hat{y}_i - \Theta_k^{(y)} \phi_i \right\|^2 \\ \Theta_{k,opt}^{(x)} &:= \underset{\Theta_k^{(x)}}{argmin} \sum_{i=k-m_p}^{k} \left\| \hat{x}_i - \Theta_k^{(x)} \psi_i \right\|^2. \end{aligned} \tag{A.11}$$

The algorithm in Appendix B is proposed by Houtzager et al. (2011) to recursively estimate the state variables and extracted state-space matrices from the solution of the above optimization problems.

Appendix B. - Recursive predictor-based subspace identification of the state-space matrices

Input Design Parameters: Input parameters: m_p, m_f, s.t. $m_f < m_p$, $0 < n_x$, scalars $0 < \delta_{1,2,3}$ and forgetting factors $0 \ll \lambda_{1,2,3} \leq 1$.***Initialization:*** Initialize the covariance error matrices $P_{-1} = \left(1/\delta_1\right) I_{m_p+1}$, $M_{-1} = \left(I_{n_x+n_u+n_y}/\delta_2\right)$, and $N_{-1} = \left(I_{n_x+n_u+n_y}/\delta_3\right)$.***Updating Markov Parameters:*** $P_k = \left(1/\lambda_1\right) P_{k-1} \left(I - \varphi_k \left(\lambda_1 I + \varphi_k^T P_{k-1} \varphi_k\right)^{-1} \right) \times \varphi_k^T P_{k-1}$, $\Theta_k = \Theta_{k-1} + \left(y_k - \Theta_{k-1}\varphi_k\right) \varphi_k^T P_k$.***Estimating State Variables:***. Calculate $\widetilde{\Gamma}_k \widetilde{\mathscr{L}}_k$ and $\widetilde{\Gamma}_k \widetilde{\mathscr{K}}_k$ from the updated Markov parameters Θ_k and construct $\widetilde{\mathscr{K}}_k$ by using (A.4). Update the selection matrix S_k as shown in Yang (1995):$S_k^T = S_{k-1}^T + \left(z_k - S_{k-1}^T S_{k-1} z_k\right) z_k^T P_{S,k}$. or employ the efficient propagator approach proposed by Mercére, Bako, and Lecèuche (2008) to design a stationary matrix S.

Estimate state variables from $\hat{x}_{k|k-1} = S\widetilde{\mathscr{K}}_k^{-1} \left(\widetilde{\mathscr{L}}\bar{u}_{k-m_p} + \widetilde{\mathscr{K}}\bar{y}_{k-m_p|k-m_p} \right)$***Updating State-Space Matrices*** C_k, D_k. $M_k = \left(1/\lambda_2\right) M_{k-1} - \left(1/\lambda_2\right) M_{k-1}\phi_{k-1} \times \left(\lambda_2 I + \phi_{k-1}^T M_{k-1} \phi_{k-1}\right)^{-1} \phi_{k-1}^T M_{k-1}$. $\Theta_k^{(y)} = \Theta_{k-1}^{(y)} + \left(y_{k-1} - \Theta_{k-1}^{(y)}\phi_{k-1}\right) \phi_{k-1}^T M_k$.***Updating state-space matrices*** A_k, B_k, K_k. $N_k = \left(1/\lambda_3\right) N_{k-1} - \left(1/\lambda_3\right) N_{k-1}\psi_{k-1} \times \left(\lambda_3 I + \psi_{k-1}^T N_{k-1} \psi_{k-1}\right)^{-1} \psi_{k-1}^T N_{k-1}$.. $\Theta_k^{(x)} = \Theta_{k-1}^{(x)} + \left(x_k - \Theta_{k-1}^{(x)}\psi_{k-1}\right) \psi_{k-1}^T N_k$

Appendix C. – Dynamic latent variable regression

The following algorithm is suggested by Zhu et al. (2020) for establishing correlation between the each samples of input matrix $\mathscr{X}_L$ and $s+1$ ahead samples of the output matrix $\mathscr{Y}_L$.

Updating the Data: At the current sample time $k, k = 0, 1, 2 \ldots$ drop the last row (or the last $L_s \geq 1$ samples) of the matrix $\mathscr{X}$ and augment newly L_s recorded samples to the matrix $\mathscr{X}$ to construct lagged matrices X_i and Y_s.***Normalization:*** Apply recursive mean and variance formula to update the average and standard deviation of updated data-set and to zero-center and scale matrices $\mathscr{X}_L$ and $\mathscr{Y}_L$.***Initialization:*****If** $k = 0$: Initialize β_0^i with $\frac{1}{\sqrt{s+1}}[1, \ldots, 1]$ and $u_{s,0}^{(i)}$ with a random column of Y_s.

Otherwise: Initialize $u_{s,k}^{(i)}, i = 1, ., l$ and $\beta_k^{(i)}$ with the $i-th$ column of $U_{s,k-1}$ and $\beta_{k-1}^{(i)}$, respectively.***Calculating Markov Parameters:*** Construct $X_\beta = \sum_{j=0}^{s} \beta_{k,j}^{(i)} X_{s-j}$.

Extract U_β, S_β, and V_β from singular value decomposition of X_β.

Calculate the weight vector $w^{(i)} = V_\beta \left(S_\beta^T S_\beta + \kappa I \right)^{-1} S_\beta^T U_\beta^T u_{s,k}^{(i)}$, $w^{(i)} = \frac{w^{(i)}}{\left\| X_\beta w^{(i)} \right\|}$.

Let $t^{(i)} = \mathscr{X}_L w^{(i)}$ and $T_s = \left[t_s, t_{s-1}, \ldots, t_0\right]$

Calculate the regularization factor $\kappa_w = \kappa \left\| w^{(i)} \right\|^2$ and find the eigenvector q corresponding to the maximum eigenvalue of $Y_s^T T_s \left(T_s^T T_s + \kappa_w I \right)^{-1} T_s^T Y_s$.

Update $u_{s,k}^{(i)} = Y_s q$ and $\beta_k^{(i)} = \left(T_s^T T_s + \kappa_w I \right)^{-1} T_s^T u_{s,k}^{(i)}$. and normalize it by $\beta_k^{(i)} = \frac{\beta_k^{(i)}}{\left\| \beta_k^{(i)} \right\|}$

Iterate previous steps until $u_{s,k}^{(i)}$ and $\beta_k^{(i)}$ converge and at each iteration, check the relative error of $\beta_k^{(i)}$.

Rescale $\beta_k^{(i)}$ to calculate inner parameter $\alpha^{(i)}$ as $\alpha^{(i)} = \left(T_s^T T_s + \kappa_w I \right)^{-1} T_s^T u_{s,k}^{(i)}$***Deflation:*** Deflate matrices $\mathscr{X}_L$ and $\mathscr{Y}_s$ as

$\hat{u}_s^{(i)} = T_s \alpha^{(i)}$, $p^{(i)} = \frac{\mathscr{X}_L t^{(i)}}{\left\| t^{(i)} \right\|^2}$, $c^{(i)} = \frac{\mathscr{Y}_s \hat{u}_s^{(i)}}{\left\| \hat{u}_s^{(i)} \right\|^2}$

$U_{s,k} = \left[U_{s,k}, u_{s,k}^{(i)} \right]$

$\mathscr{P} = \left[\mathscr{P}, p^{(i)} \right]$

$\mathscr{W} = \left[\mathscr{W}, w^{(i)} \right]$

$\mathscr{C} = \left[\mathscr{C}, c^{(i)} \right]$

$\hat{U}_s = \left[\hat{U}_s, \hat{u}_s^{(i)} \right]$

$\mathscr{T} = \left[\mathscr{T}, t^{(i)} \right]$

$\mathscr{X}_L := \mathscr{X}_L - t^{(i)} p^{(i)T}$

$\mathscr{Y}_s := \mathscr{Y}_s - \hat{u}_s c^{(i)T}$

Repeat the procedure starting from initialization step until all l latent variables are extracted.

References

Basila Jr, M.R., Cinar, A., & Stefanek, G. (1989). Mobecs: Model-object based expert control systems. IFAC Proceedings Volumes, 22(8), 163–168.

Breton, M.D. (2008). Physical activity-the major unaccounted impediment to closed loop control. Journal of Diabetes Science and Technology, 2(1), 169–174.

Cheung, J.T.Y., & Stephanopoulos, G. (1990). Representation of process trends-part I. A formal representation framework. Computers & Chemical Engineering, 14(4–5), 495–510.

Chiuso, A., & Picci, G. (2005). Consistency analysis of some closed-loop subspace identification methods. Automatica, 41(3), 377–391.

Chou, C.T., & Verhaegen, M. (1997). Subspace algorithms for the identification of multivariable dynamic errors-in-variables models. Automatica, 33(10), 1857–1869.

Dong, Y., & Qin, S.J. (2018). A novel dynamic PCA algorithm for dynamic data modeling and process monitoring. Journal of Process Control, 67, 1–11.

M.G. Forbes R.S. Patwardhan H. Hamadah R.B. Gopaluni Model predictive control in industry: Challenges and opportunities IFAC-Papers OnLine 48 8 2015 531 538 9th IFAC Symposium on Advanced Control of Chemical Processes ADCHEM 2015

Galassetti, P., & Riddell, M.C. (2013). Exercise and type 1 diabetes (t1dm). Comprehensive Physiology, 3(3), 1309–1336.

Ganesh, H., Edgar, T., & Baldea, M. (2016). Model predictive control of the exit part temperature for an austenitization furnace. Processes, 4(4), 53.
Garcia, C.E., Prett, D.M., & Morari, M. (1989). Model predictive control: Theory and practice–a survey. Automatica, 25(3), 335–348.
Garcia-Tirado, J., Corbett, J.P., Boiroux, D., Jørgensen, J.B., & Breton, M.D. (2019). Closed-loop control with unannounced exercise for adults with type 1 diabetes using the ensemble model predictive control. Journal of Process Control, 80, 202–210.
Gensym, C. (1996). G2 Reference Manual. MA: Gensym Corporation Cambridge.
Hajizadeh, I., Askari, M.R., Kumar, R., Zavala, V.M., & Cinar, A. (2020 (in press)). Integrating MPC with learning-based and adaptive methods to enhance safety, performance and reliability in automated insulin delivery. IFAC Proceedings Volumes.
Hajizadeh, I., Hobbs, N., Samadi, S., Sevil, M., Rashid, M., Brandt, R., … Cinar, A. (2019). Controlling the ap controller: Controller performance assessment and modification. Journal of Diabetes Science and Technology, 13(6), 1091–1104.
Hajizadeh, I., Rashid, M., & Cinar, A. (2018). Integrating compartment models with recursive system identification. 2018 annual American control conference (ACC) (pp. 3583–3588). IEEE.
Hajizadeh, I., Rashid, M., & Cinar, A. (2019). Plasma-insulin-cognizant adaptive model predictive control for artificial pancreas systems. Journal of Process Control, 77, 97–113.
Hajizadeh, I., Rashid, M., Samadi, S., Sevil, M., Hobbs, N., Brandt, R., & Cinar, A. (2019). Adaptive personalized multivariable artificial pancreas using plasma insulin estimates. Journal of Process Control, 80, 26–40.
Hajizadeh, I., Rashid, M., Turksoy, K., Samadi, S., Feng, J., Sevil, M., … Cinar, A. (2018). Incorporating unannounced meals and exercise in adaptive learning of personalized models for multivariable artificial pancreas systems. Journal of Diabetes Science and Technology, 12(5), 953–966.
Hajizadeh, I., Samadi, S., Sevil, M., Rashid, M., & Cinar, A. (2019). Performance assessment and modification of an adaptive model predictive control for automated insulin delivery by a multivariable artificial pancreas. Industrial & Engineering Chemistry Research, 58(26), 11506–11520.
Houtzager, I., van Wingerden, J.-W., & Verhaegen, M. (2011). Recursive predictor-based subspace identification with application to the real-time closed-loop tracking of flutter. IEEE Transactions on Control Systems Technology, 20(4), 934–949.
Hovorka, R., Canonico, V., Chassin, L.J., Haueter, U., Massi-Benedetti, M., Federici, M.O., … Vering, T., et al. (2004). Nonlinear model predictive control of glucose concentration in subjects with type 1 diabetes. Physiological Measurement, 25(4), 905.
Kendra, S.J., Basila, M.R., & Cinar, A. (1994). Intelligent process control with supervisory knowledge-based systems. IEEE Control Systems Magazine, 14(3), 37–47.
Kendra, S.J., Basila, M.R., & Cinar, A. (1997). A supervisory kbs for real-time monitoring and modification of multivariable controllers for continuous processes. In methods and applications of intelligent control (pp. 139–171). Springer Science & Business Media.
Kumar, R., Jalving, J., Wenzel, M.J., Ellis, M.J., ElBsat, M.N., Drees, K.H., & Zavala, V.M. (2019). Benchmarking stochastic and deterministic MPC: A case study in stationary battery systems. AIChE Journal, 65(7), e16551.
Kumar, R., Wenzel, M.J., Ellis, M.J., ElBsat, M.N., Drees, K.H., & Zavala, V.M. (2018). A stochastic model predictive control framework for stationary battery systems. IEEE Transactions on Power Systems, 33(4), 4397–4406.
Kumar, R., Wenzel, M.J., Ellis, M.J., ElBsat, M.N., Drees, K.H., & Zavala, V.M. (2019). Hierarchical MPC schemes for periodic systems using stochastic programming. Automatica, 107, 306–316.
Lennart, L. (1999). System identification: Theory for the user. PTR Prentice Hall, Upper Saddle River, NJ, 1–14.
Loehlin, J.C., & Beaujean, A.A. (2016). Latent variable models: An introduction to factor, path, and structural equation analysis. Taylor & Francis.
Maurya, M.R., Rengaswamy, R., & Venkatasubramanian, V. (2005). Fault diagnosis by qualitative trend analysis of the principal components. Chemical Engineering Research and Design, 83(9), 1122–1132.
Mayne, D.Q. (2014). Model predictive control: Recent developments and future promise. Automatica, 50(12), 2967–2986.
Mercére, G., Bako, L., & Lecèuche, S. (2008). Propagator-based methods for recursive subspace model identification. Signal Processing, 88(3), 468–491.
Mesbah, A. (2016). Stochastic model predictive control: An overview and perspectives for future research. IEEE Control Systems Magazine, 36(6), 30–44.
Mesbah, A., Paulson, J.A., Lakerveld, R., & Braatz, R.D. (2017). Model predictive control of an integrated continuous pharmaceutical manufacturing pilot plant. Organic Process Research & Development, 21(6), 844–854.
Moharir, M., Pourkargar, D.B., Almansoori, A., & Daoutidis, P. (2018). Distributed model predictive control of an amine gas sweetening plant. Industrial & Engineering Chemistry Research, 57(39), 13103–13115.
Oku, H., & Kimura, H. (2002). Recursive 4sid algorithms using gradient type subspace tracking. Automatica, 38(6), 1035–1043.
Perea-Lopez, E., Ydstie, B.E., & Grossmann, I.E. (2003). A model predictive control strategy for supply chain optimization. Computers & Chemical Engineering, 27(8–9), 1201–1218.
Perk, S., Shao, Q.M., Teymour, F., & Cinar, A. (2012). An adaptive fault-tolerant control framework with agent-based systems. International Journal of Robust and Nonlinear Control, 22(1), 43–67.
Perk, S., Teymour, F., & Cinar, A. (2011). Adaptive agent-based system for process fault diagnosis. Industrial & Engineering Chemistry Research, 50(15), 9138–9155.
Qin, S.J. (2006). An overview of subspace identification. Computers & Chemical Engineering, 30(10–12), 1502–1513.
Rashid, M., Samadi, S., Sevil, M., Hajizadeh, I., Kolodziej, P., Hobbs, N., … Cinar, A. (2019). Simulation software for assessment of nonlinear and adaptive multivariable control algorithms: Glucose-insulin dynamics in Type 1 diabetes. Computers & Chemical Engineering, 130, 106565.
Rawlings, J.B., & Mayne, D.Q. (2009). Model predictive control: Theory and design. Nob Hill Pub..
Reddy, M., Herrero, P., Sharkawy, M.E., Pesl, P., Jugnee, N., Pavitt, D., … Johnston, D.G., et al. (2016). Metabolic control with the bio-inspired artificial pancreas in adults with type 1 diabetes: A 24-hour randomized controlled crossover study. Journal of Diabetes Science and Technology, 10(2), 405–413.
Riddell, M., & Perkins, B.A. (2009). Exercise and glucose metabolism in persons with diabetes mellitus: Perspectives on the role for continuous glucose monitoring. Journal of Diabetes Science and Technology, 3(4), 914–923.
Ripaccioli, G., Bernardini, D., Di Cairano, S., Bemporad, A., & Kolmanovsky, I. (2010). A stochastic model predictive control approach for series hybrid electric vehicle power management. Proceedings of the 2010 American control conference (pp. 5844–5849). IEEE.
Samadi, S., Rashid, M., Turksoy, K., Feng, J., Hajizadeh, I., Hobbs, N., … Cinar, A. (2018). Automatic detection and estimation of unannounced meals for multivariable artificial pancreas system. Diabetes Technology & Therapeutics, 20(3), 235–246.
Samadi, S., Turksoy, K., Hajizadeh, I., Feng, J., Sevil, M., & Cinar, A. (2017). Meal detection and carbohydrate estimation using continuous glucose sensor data. IEEE journal of Biomedical and Health Informatics, 21(3), 619–627.
Schäfer, J., & Cinar, A. (2004). Multivariable MPC system performance assessment, monitoring, and diagnosis. Journal of Process Control, 14(2), 113–129.
Sevil, M., Rashid, M., Hajizadeh, I., Maloney, Z., Samadi, S., Askari, M.R., … Cinar, A. (2019). Assessing the effects of stress response on glucose variations. 2019 IEEE 16th international conference on wearable and implantable body sensor networks (BSN) (pp. 1–4).
M. Sevil M. Rashid Z. Maloney I. Hajizadeh S. Samadi M.R. Askari ... A. Cinar Determining physical activity characteristics from wristband data for use in automated insulin delivery systems IEEE Sensors Journal 2020
1–1
Tatara, E., & Cinar, A. (2002). An intelligent system for multivariate statistical process monitoring and diagnosis. ISA Transactions, 41(2), 255–270.
Tatara, E., North, M., Hood, C., Teymour, F., & Cinar, A. (2005). Agent-based control of spatially distributed chemical reactor networks. International workshop on engineering self-organising applications (pp. 222–231). Springer.
Thabit, H., & Hovorka, R. (2016). Coming of age: The artificial pancreas for type 1 diabetes. Diabetologia, 59(9), 1795–1805.
Turksoy, K., Bayrak, E.S., Quinn, L., Littlejohn, E., & Cinar, A. (2013). Multivariable adaptive closed-loop control of an artificial pancreas without meal and activity announcement. Diabetes Technology & Therapeutics, 15(5), 386–400.
Turksoy, K., Quinn, L., Littlejohn, E., & Cinar, A. (2013). Multivariable adaptive identification and control for artificial pancreas systems. IEEE Transactions on Biomedical Engineering, 61(3), 883–891.
Velu, R., & Reinsel, G.C. (2013). Multivariate reduced-rank regression: Theory and applications (136). Springer Science & Business Media.
Verhaegen, M. (1993). Application of a subspace model identification technique to identify LTI systems operating in closed-loop. Automatica, 29(4), 1027–1040.
Wang, J., & Qin, S.J. (2002). A new subspace identification approach based on principal component analysis. Journal of Process Control, 12(8), 841–855.
Yang, B. (1995). Projection approximation subspace tracking. IEEE Transactions on Signal Processing, 43(1), 95–107.
Zavala, V.M., & Biegler, L.T. (2009). The advanced-step NMPC controller: Optimality, stability and robustness. Automatica, 45(1), 86–93.
Zecchin, C., Facchinetti, A., Sparacino, G., Dalla Man, C., Manohar, C., Levine, J.A., … Cobelli, C. (2013). Physical activity measured by physical activity monitoring system correlates with glucose trends reconstructed from continuous glucose monitoring. Diabetes Technology & Therapeutics, 15(10), 836–844.
Zhou, L., Li, G., Song, Z., & Qin, S.J. (2016). Autoregressive dynamic latent variable models for process monitoring. IEEE Transactions on Control Systems Technology, 25(1), 366–373.
Zhu, Q., Liu, Q., & Qin, S.J. (2017). Concurrent quality and process monitoring with canonical correlation analysis. Journal of Process Control, 60, 95–103.
Zhu, Q., Qin, S.J., & Dong, Y. (2020). Dynamic latent variable regression for inferential sensor modeling and monitoring. Computers & Chemical Engineering, 106809.